Particle creation and entanglement in a dispersive model with step velocity profile

Yuki Osawa[*] and Yasusada Nambu[†]

Department of Physics, Nagoya University, Nagoya 464-8602, Japan

(Received 10 February 2023; accepted 20 April 2023; published 10 May 2023)

We investigate particle creation and entanglement structure in a dispersive model with subluminal dispersion relation. Assuming the step function spatial velocity profile of the background flow, mode functions for a massless scalar field are exactly obtained by the matching method. Power spectrums of created particles are calculated for the subsonic and the trans-sonic flow cases. For the trans-sonic case, the sonic horizon exists, and created particles show the Planckian distribution for the low frequency region, but the thermal property disappears for the high frequency region near the cutoff frequency introduced by the nonlinear dispersion. For the subsonic case, although the sonic horizon does not exist, the effective group velocity horizon appears due to the nonlinear dispersion for the high frequency region, and an approximate thermal property of the power spectrum arises. The relation between particle creation and entanglement between each mode is also discussed.

DOI: 10.1103/PhysRevD.107.105005

I. INTRODUCTION

Quantum field theory in black hole spacetimes predicts the emission of thermal Hawking radiation from black holes, whose temperature is given by the surface gravity at their event horizons [1,2]. This property of Hawking radiation from black holes suggests that black holes behave as a kind of thermodynamical object, and the theory of black hole thermodynamics is formulated [3]. The thermal property of Hawking radiation leads to a problem called the information loss paradox, and for deeper understanding of this issue, an analysis of entanglement between the Hawking mode (Hawking radiation) and its partner mode has been done to investigate the quantum informational aspect of the black hole evaporation [4].

The original Hawking's scenario implies that low energy radiations are originated from a high energy region above the Planckian scale, at which quantum gravitational physics will become important. Thus it is crucial to clarify the effect of the Planckian scale cutoff on the thermal property of Hawking radiation (the trans-Planckian problem) [5,6]. To resolve this problem, it is necessary to consider the origin of the particle radiated from the black hole. If we consider time reversed evolution of emission of Hawking radiation, the frequency of emitted radiations exponentially increases as they approach the black hole horizon and exceeds the Planckian frequency; beyond the frequency, the quantum effect of gravity may become important. To investigate such a situation, Unruh proposed a sonic analog of black holes [7,8]; he found that the equation of sonic waves in moving fluid has the same form as a massless scalar field in curved spacetimes, whose metric has a similar structure as black hole spacetimes. The acoustic metric corresponds to the black hole spacetime with Painlevé coordinates

$$ds^2 = -c^2dt^2 + (dx - v(x)dt)^2, \qquad v(x) = -c\sqrt{x_s/x} \quad (1)$$

where x_s is the Schwarzschild radius and c is the light velocity. A cutoff wave number k_0 is introduced as the distance between atoms constituting fluid. He numerically calculated the power spectrum of the radiation for the analog black hole with the high frequency cutoff and has shown that the cutoff does not affect the spectrum of Hawking radiation in a low frequency region.

Owing to the introduction of the frequency cutoff, the Lorentz invariance of the system is broken, and additional wave modes associated with the cutoff appear. Owing to these modes, Hawking radiation in analog black holes is produced by a process that the Planckian modes transformed into the low energy modes (mode conversion). If the velocity profile $v(x)$ is a slowly changing function of the spatial coordinate, a lot of analyses have been done so far based on the WKB method. These studies show that for $\omega, \kappa \ll k_0$ where κ is the first derivative of the velocity profile at the sonic horizon, the temperature of the radiation is given by $\kappa/(2\pi)$, and this coincides with Hawking's results [6,9–12].

If the velocity profile $v(x)$ is not a slowly changing function of the spatial coordinate, and if the expected temperature of analog black holes is high, then several studies of particle creation in analog models [11,13–16]

[*]osawa.yuki.e8@s.mail.nagoya-u.ac.jp
[†]nambu@gravity.phys.nagoya-u.ac.jp

have shown that the spectrum of radiation depends not only on the first derivative of the fluid velocity at the sonic horizon, but also on other parameters such as the frequency cutoff. This implies that the mechanism of radiation from analog black holes with high temperature does differs from the original Hawking radiation. Investigations of entanglement for analog models of black holes also have been done recently [17–20]. The study of the entanglement between involved modes is useful not only for the detection of the Hawking radiation in the laboratory experiment but also for understanding the emission mechanism of the radiation. In this paper, we consider an analog model with a step function velocity profile of the background flow, and apply the step discontinuous method introduced by [11,13,15] to evaluate Bogoliubov coefficients. Then we calculate the number density of created particles and entanglement negativity between involved modes. Although the present study may have overlaps with the analysis by Busch and Parentani [17], in which entanglement structure for a high temperature analog black hole was studied, our analysis differs from their work in several points; first, we calculated the multipartite entanglement between modes. Second, we investigated the structure of partner modes for two different types of analog spacetimes: the one with a sonic horizon and the other without a sonic horizon.

The paper is organized as follows. In Sec. II, we shortly review particle creation in an analog system with the dispersive media. In Sec. III, we determine the Bogoliubov coefficients for the step function velocity profile. In Sec. IV, we investigate the entanglement structure of the in-vacuum state. In Sec. V, we show the results of our numerical calculation. Section VI is devoted to the summary and conclusion. We used the unit $c = \hbar = G = 1$ throughout this paper.

II. WAVE MODES FOR STEEP VELOCITY PROFILE

We consider wave modes of an analog model with dispersive media. This section is mainly based on [11,12]. We adopt the following wave equation of a massless real scalar field [8,12]:

$$(\partial_t + \partial_x v(x))(\partial_t + v(x)\partial_x)\phi(x,t) = c_s^2(-i\partial_x)\partial_x^2\phi(x,t). \tag{2}$$

This is the equation for sonic waves in a moving fluid with a position dependent velocity profile $v(x)$ and the sound velocity $c_s(k)$ with the wave number $k = -i\partial_x$. In the following, we assume that the velocity of the fluid has the step function profile[1]

$$v(x) = V_- + (V_+ - V_-)\theta(x), \qquad V_\pm < 0, \tag{3}$$

and the flow velocity in the $x > 0$ region is subsonic $V_+ > -1$. We assume subluminal dispersion $c_s^2(k) = 1 - k^2/k_0^2$ with the cutoff of wave number k_0. This type of dispersion arises from the dispersion relation for a chain of harmonic oscillators, $\omega^2 \propto \sin^2(ka/2)$, where a is the parameter related to the distance between particles. This dispersion relation has also been observed in dc-SQUID systems [21,22]. The sonic horizon exists at $x = 0$ if $V_- < -1$, and in such a case, the region $x < 0$ becomes supersonic (inside of the sonic horizon). We will see in Sec. II A that, owing to the dispersive property of the fluid for high frequency, there exists an effective horizon (group velocity horizon) that has a similar property to the sonic horizon, even when the whole region is subsonic and there is no sonic horizon.

A. Mode functions

For the wave equation (2) with the subluminal dispersion and the velocity profile, Eq. (3), by assuming $\phi \propto e^{-i\omega t + ikx}(x \neq 0)$, the dispersion relation is obtained as

$$\omega - kV_\pm = \pm|k|\sqrt{1 - \left(\frac{k}{k_0}\right)^2}, \qquad \omega > 0. \quad \text{(signs in no particular order)} \tag{4}$$

We denote $k_i^\pm(\omega)$ as solutions of the dispersion relation corresponding to $V_\pm$, where the index i denotes a label to distinguish modes. Since the spacetime is static and the wave equation does not contain explicit time dependence, a plane wave with a frequency ω does not couple to other plane waves with different ω. We call ω the laboratory frequency and $\Omega := \omega - kV_\pm$ the comoving frequency. Note that the comoving frequency is not conserved and changes its value depending on x. Solutions of the dispersion relation and corresponding modes in our setup are shown in Fig. 1 using a dispersion diagram; the vertical axis is the comoving frequency and the horizontal axis is the wave number. The

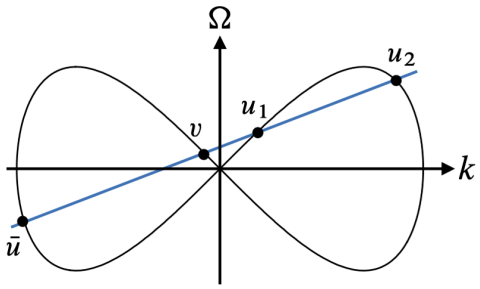

FIG. 1. Dispersion diagram with the subluminal dispersion for the subsonic case. A straight line represents $\Omega = \omega - V_\pm k$. The dispersion relation has four roots which define modes. We name them $\bar{u}, v, u_1, u_2$ modes in the increasing order of k.

[1]The step function is defined by

$$\theta(x) = \begin{cases} 0 & (x < 0) \\ 1/2 & (x = 0) \\ 1 & (x > 0)\,. \end{cases}$$

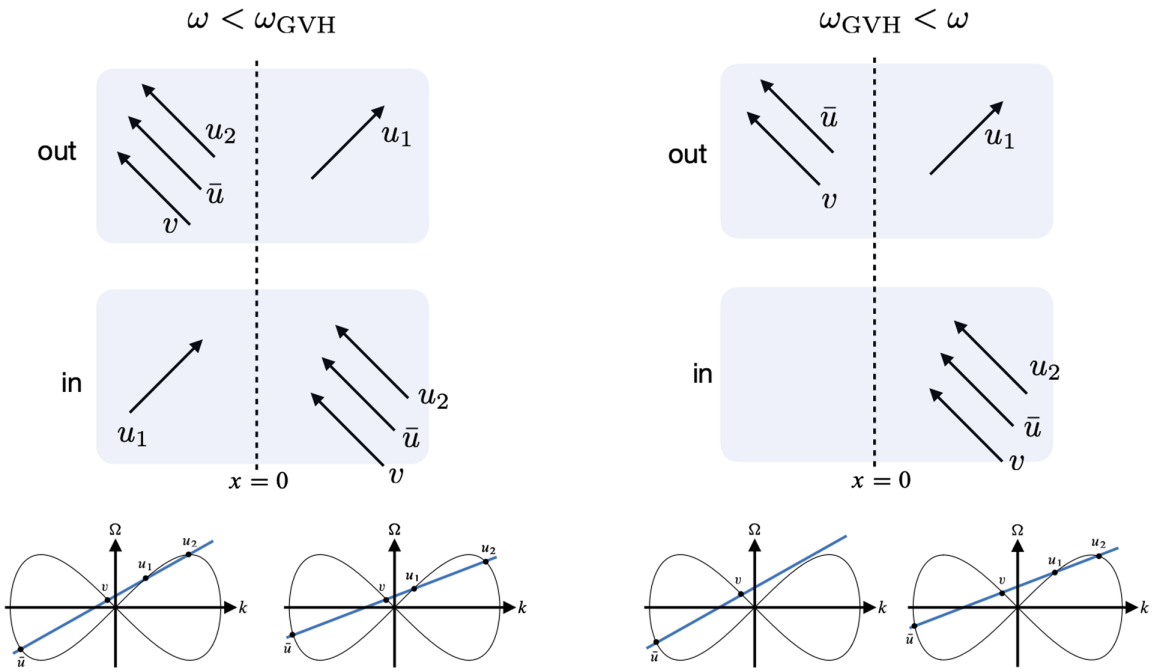

FIG. 2. Dispersion diagrams and modes for the subsonic case. For $\omega < \omega_{\mathrm{GVH}}$, the in-state and the out-state contain independent four modes. For $\omega_{\mathrm{GVH}} < \omega$, there in no right-moving modes in $x < 0$ and the in-state and the out-state contain three independent modes.

curve in the diagram represents the right-hand side of the dispersion relation $\pm|k|\sqrt{1-(k/k_0)^2}$, and the straight line represents the left-hand side of the dispersion relation $\omega - kV_{\pm}$.

From this diagram, we can identify modes as four real roots $k_{\bar{u}}, k_v, k_{u_1}, k_{u_2}$ in the increasing order of k. For larger values of ω or $|V_{\pm}|$, we will have only two real solutions, $k_{\bar{u}}, k_v$ with $k < 0$, and two nonreal solutions. One of the imaginary solutions corresponds to the decaying mode, and the other imaginary solution corresponds to the growing mode. For the velocity profile with the step function (3), mode functions $\phi_i^{\pm}$ are plane waves

$$\phi^{\pm}_{\omega,i}(t,x) = e^{-i\omega t} C^{\pm}_{\omega,i} \exp\left(ik^{\pm}_i(\omega)x\right), \quad i = \bar{u}, v, u_1, u_2, \quad (5)$$

where the index $\pm$ corresponds to the sign of the x coordinate, and $C^{\pm}_{\omega,i}$ are normalization constants. We call $u_2, \bar{u}$ in $x > 0$ Planckian modes and v, u_1 in $x > 0$, and $\bar{u}$ in $x < 0$ non-Planckian modes. The Planckian modes appear due to nonlinearity of the dispersion relation. On the other hand, the non-Planckian modes exist even for linear dispersion without the cutoff effect. The naming of modes depends on values of ω and $V_{\pm}$. With the increase of ω, the non-Planckian mode u_1 approaches the Planckian u_2 mode. In such a situation, we call u_1 the sub-Planckian mode. The group velocity of each mode is given by

$$v_g = \left(\frac{dk(\omega)}{d\omega}\right)^{-1}. \quad (6)$$

We present behavior of modes for the subsonic case (Fig. 2) and the trans-sonic case (Fig. 3). The in modes are defined as modes with negative group velocity for $x > 0$ and positive group velocity for $x < 0$ (incoming to $x = 0$ from $x = \pm\infty$). The out modes are defined as modes with positive group velocity for $x > 0$ and negative group velocity for $x < 0$ (outgoing from $x = 0$ toward $x = \pm\infty$).

For the subsonic case (Fig. 2), we assume $-1 < V_- < V_+ < 0$. For sufficiently small ω, there are four in and out

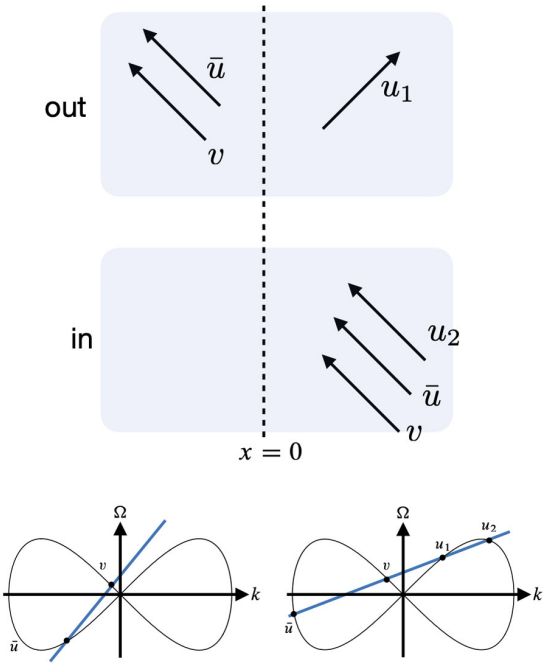

FIG. 3. Dispersion diagrams and modes for the trans-sonic case. There are no right-moving modes in $x < 0$.

modes (left panel in Fig. 2). If we increase ω, the mode u_1 and the mode u_2 in $x < 0$ coalesce at the critical frequency $\omega_{\rm GVH}$, and above this frequency, we have only two out modes in $x < 0$ (right panel in Fig. 2). For $\omega_{\rm GVH} < \omega$, $x = 0$ behaves as a sonic horizon because there exist no right-moving modes in $x < 0$, and this region effectively becomes the supersonic region. We call this effective horizon the group velocity horizon (GVH) [11]. There are three in modes in $x > 0$ ($u_2, \bar{u}, v$), and one out mode for $x > 0$ (u_1) and two out modes in $x < 0$ ($\bar{u}, v$).

For the trans-sonic case $V_- < -1 < V_+ < 0$ (Fig. 3), $x = 0$ is the sonic horizon. There are three in modes in $x > 0$ ($u_2, \bar{u}, v$), and two out modes in $x < 0$ ($\bar{u}, v$) and one out mode for $x > 0$ (u_1). There exist no right-moving modes in the supersonic region $x < 0$.

The incoming Planckian mode u_2^+ is reflected at the sonic horizon or the GVH. And it is transformed to the outgoing sub-Planckian mode u_1^+. This process is called the mode conversion [12]. At the same time, the Planckian mode $\bar{u}^+$ is transformed to the sub-Planckian mode $\bar{u}^-$ for the trans-sonic case. More detailed discussion on modes for the slowly varying velocity profile can be found in [9–11].

B. Quantization and vacuum state

We quantize a classical field obeying the field equation Eq. (2). The action for the field is given by

$$S = \int dtdx[|(\partial_t + v\partial_x)\phi|^2 - |c_s(i\partial_x)\partial_x\phi|^2], \tag{7}$$

and the conjugate momentum $\pi(t,x)$ for $\phi(t,x)$ is given by

$$\pi(t,x) = (\partial_t + v\partial_x)\phi(t,x). \tag{8}$$

The canonical commutation relation between quantized fields is imposed as

$$[\hat{\phi}(t,x), \hat{\pi}(t,y)] = i\delta(x-y). \tag{9}$$

The Klein-Gordon inner product [12] on $t =$ const surface for solutions ϕ_1, ϕ_2 of the field equation is defined by

$$\begin{aligned}(\phi_1, \phi_2) &:= -i\int dx(\phi_1 D\phi_2^* - \phi_2^* D\phi_1) \\ &= -i\int_\Sigma dx(\phi_1\pi_2^* - \phi_2^*\pi_1),\end{aligned} \tag{10}$$

where $D = \partial_t + v\partial_x$ and the inner product is conserved:

$$\frac{d(\phi_1,\phi_2)}{dt} = 0. \tag{11}$$

With the Klein-Gordon inner product, we can define creation and annihilation operators associated with the positive norm solution $\{\phi_i\}$ of the wave equation by

$$\hat{a}(\phi_i) = (\phi_i, \hat{\phi}), \qquad \hat{a}^\dagger(\phi_i) = -(\phi_i^*, \hat{\phi}). \tag{12}$$

This set of creation and annihilation operators satisfies the following commutation relations:

$$\begin{aligned}[\hat{a}(\phi_i), \hat{a}^\dagger(\phi_j)] &= (\phi_i, \phi_j), \\ [\hat{a}(\phi_i), \hat{a}(\phi_j)] &= -(\phi_i, \phi_j^*), \\ [\hat{a}^\dagger(\phi_i), \hat{a}^\dagger(\phi_j)] &= -(\phi_i^*, \phi_j).\end{aligned} \tag{13}$$

Thus if we choose a basis with an orthonormal condition, our creation and annihilation operators satisfy the standard commutation relation for the creation and annihilation operators. In general, it is not easy to construct exactly the orthonormal basis with respect to the Klein-Gordon inner product. However, for the step function velocity profile, as all modes are represented by plane waves, it is easy to identify positive frequency modes which define a vacuum state. We note that the mode functions for $\bar{u}^\pm$ have negative norms and other modes have positive norms. Once we defined a vacuum state, multiparticle states can be obtained by acting the creation operator on the vacuum state. We have two kinds of vacuum states. The in-vacuum state $|0_{\rm in}\rangle$ is the state with no particle at $t \to -\infty, x \to \pm\infty$

$$\hat{a}(\phi_i^{\rm in})|0_{\rm in}\rangle = 0, \tag{14}$$

where $\phi_i^{\rm in}$ is the positive frequency mode function of the in-state for $i = u_1^-, \bar{u}^+, v^+, u_2^+$ (subsonic case with $\omega < \omega_{\rm int}$), and $i = u_2^+, \bar{u}^+, v^+$ (subsonic case with $\omega_{\rm int} < \omega$ or trans-sonic case). The out-vacuum state $|0_{\rm out}\rangle$ is the state with no particle at $t \to +\infty, x \to \pm\infty$,

$$\hat{a}(\phi_i^{\rm out})|0_{\rm out}\rangle = 0, \tag{15}$$

where $\phi_i^{\rm out}$ is the positive frequency mode function of the out-state for $i = \bar{u}^-, v^-, u_2^-, u_1^+$ (subsonic case with $\omega < \omega_{\rm int}$), and $i = \bar{u}^-, v^-, u_1^+$ (subsonic case with $\omega_{\rm int} < \omega$ or trans-sonic case). In general, these two vacuum states are not equal, and the number of the out-state particles in the in-state vacuum is

$$\langle 0_{\rm in}|\hat{a}^\dagger(\phi_i^{\rm out})\hat{a}(\phi_i^{\rm out})|0_{\rm in}\rangle \neq 0. \tag{16}$$

This implies particle creation occurs at $x = 0$.

The field operator is expanded as

$$\begin{aligned}\hat{\phi}(t,x) &= \sum_i (\hat{a}(\phi_i^{\rm in})\phi_i^{\rm in} + ({\rm H.c.})) \\ &= \sum_i (\hat{a}(\phi_i^{\rm out})\phi_i^{\rm out} + ({\rm H.c.})),\end{aligned} \tag{17}$$

and creation and annihilation operators are represented as

$$\hat{a}(\phi_i^{\rm in,out}) = (\phi_i^{\rm in,out}, \hat{\phi}), \quad \hat{a}^\dagger(\phi_i^{\rm in,out}) = -(\phi_i^{\rm in,out_*}, \hat{\phi}). \tag{18}$$

III. BOGOLIUBOV COEFFICIENTS

We can analytically determine a relation between the in-mode state and the out-mode state for the wave equation with the step function velocity profile.

A. Matching method

By separating the time dependence of the wave function as $\propto e^{-i\omega t}$ in Eq. (2), the wave equation becomes the following ordinary differential equation:

$$(-i\omega+\partial_x v(x))(-i\omega+v(x)\partial_x)\phi(x)=\left(1+\frac{1}{k_0^2}\partial_x^2\right)\partial_x^2\phi(x) \tag{19}$$

with the velocity profile given by Eq. (3). For $x\neq 0$, the solution of this equation is the superposition of plane waves $\exp(ik_i^+x)$ for $x>0$ and $\exp(ik_i^-x)$ for $x<0$. Coefficients of superposition are determined by matching conditions at $x=0$. Let us denote $\phi_\pm$ as the solution of Eq. (19) for $x\gtrless 0$. We impose matching conditions between ϕ_+ and ϕ_- at $x=0$ as follows. We require a continuity condition of ϕ at $x=0$ up to the second spatial derivative to ensure the well-behaved wave function. An additional condition is obtained by integrating both sides of the wave equation in the range $-\varepsilon<x<\varepsilon$, and taking $\varepsilon\to 0$:

$$\begin{aligned}&-i\omega(V_+-V_-)\phi(0)+(V_+^2-V_-^2)\partial_x\phi(0)\\&\quad=\frac{1}{k_0^2}[\partial_x^3\phi^+(0)-\partial_x^3\phi^-(0)].\end{aligned} \tag{20}$$

After all, we require the following four matching conditions [11,15]:

$$\begin{aligned}&\phi^+(0)=\phi^-(0),\qquad \partial_x\phi^+(0)=\partial_x\phi^-(0),\\&\partial_x^2\phi^+(0)=\partial_x^2\phi^-(0),\\&\partial_x^3\phi^+(0)=\partial_x^3\phi^-(0)-k_0^2(V_+-V_-)\{i\omega\phi(0)\\&\qquad-(V_++V_-)\partial_x\phi(0)\}.\end{aligned} \tag{21}$$

Then the wave function $\phi(x)=\phi_+(x)\theta(x)+\phi_-(x)\theta(-x)$ is the global solution of the wave equation (19).

B. Bogoliubov coefficients

By using the matching formula, Eq. (21), we can construct $\phi_i^+(x)$ defined for $x>0$ connected to the plane wave $e^{ik_i^-x}$ for $x<0$. $\phi_i^+(x)$ can be expressed as

$$\phi_i^+(x)=\sum_{j=1}^{4}\alpha_{ij}\exp(ik_j^+x) \tag{22}$$

with superposition coefficients $\{\alpha_{ij}\}$. Wave numbers $\{k_j^+(\omega)\}$ are determined by Eq. (4). The matching formula [Eq. (21)] yields the following equations for $\{\alpha_{ij}\}$:

$$\sum_j\alpha_{ij}=1,\qquad \sum_j\alpha_{ij}k_j^+=k_i^-,\qquad \sum_j\alpha_{ij}(k_j^+)^2=(k_i^-)^2, \tag{23}$$

$$\sum_j\alpha_{ij}(k_j^+)^3=(k_i^-)^3+k_0^2(V_+-V_-)\{\omega-(V_++V_-)k_i^-\}. \tag{24}$$

By solving these relations for α_{il}, we obtain

$$\begin{aligned}\begin{pmatrix}\alpha_{i1}\\ \alpha_{i2}\\ \alpha_{i3}\\ \alpha_{i4}\end{pmatrix}&=\begin{pmatrix}-B_1/A_1 & C_1/A_1 & -D_1/A_1 & 1/A_1\\ -B_2/A_2 & C_2/A_2 & -D_2/A_2 & 1/A_2\\ -B_3/A_3 & C_3/A_3 & -D_3/A_3 & 1/A_3\\ -B_4/A_4 & C_4/A_4 & -D_4/A_4 & 1/A_4\end{pmatrix}\\&\times\begin{pmatrix}1\\ k_i^-\\ (k_i^-)^2\\ (k_i^-)^3+k_0^2(V_+-V_-)\{\omega-(V_++V_-)k_i^-\}\end{pmatrix}\end{aligned} \tag{25}$$

with

$$A_i=(k_i^+-k_j^+)(k_i^+-k_k^+)(k_i^+-k_l^+),\qquad B_i=k_j^+k_k^+k_l^+, \tag{26}$$

$$\begin{aligned}&C_i=k_j^+k_k^++k_k^+k_l^++k_l^+k_j^+,\\&D_i=k_j^++k_k^++k_l^+\\&\quad\text{(indices } i,j,k,l \text{ are different from each other)}.\end{aligned} \tag{27}$$

Bogoliubov coefficients are expressed with the superposition coefficients $\{\alpha_{ij}\}$ (see Appendix A for more details):

$$\begin{pmatrix}-(\hat{a}_{\bar{u}}^{\rm out})^\dagger\\ \hat{a}_v^{\rm out}\\ \hat{a}_{u_1}^{\rm out}\\ \hat{a}_{u_2}^{\rm out}\end{pmatrix}=\begin{pmatrix}\tilde{\beta}_{\bar{u}\bar{u}} & \tilde{\beta}_{\bar{u}v} & \tilde{\beta}_{\bar{u}u_1} & \tilde{\beta}_{\bar{u}u_2}\\ \tilde{\beta}_{v\bar{u}} & \tilde{\beta}_{uv} & \tilde{\beta}_{vu_1} & \tilde{\beta}_{vu_2}\\ \tilde{\beta}_{u_1\bar{u}} & \tilde{\beta}_{u,v} & \tilde{\beta}_{u,u_1} & \tilde{\beta}_{u_1u_2}\\ \tilde{\beta}_{u_2\bar{u}} & \tilde{\beta}_{u_2v} & \tilde{\beta}_{u_2u_1} & \tilde{\beta}_{u_2u_2}\end{pmatrix}\begin{pmatrix}-(\hat{a}_{\bar{u}}^{\rm in})^\dagger\\ \hat{a}_v^{\rm in}\\ \hat{a}_{u_1}^{\rm in}\\ \hat{a}_{u_2}^{\rm in}\end{pmatrix}, \tag{28}$$

where coefficients $\{\tilde{\beta}_{ij}\}$ are given by

$$\tilde{\beta}_{u_1i}=\begin{cases}\frac{N_i^+\alpha_{u_1i}}{N_{u_1}^+\alpha_{u_1u_1}} & (i\neq u_1)\\ \frac{N_{u_1}^-}{N_{u_1}^+\alpha_{u_1u_1}} & (i=u_1)\end{cases}, \tag{29}$$

and

$$\tilde{\beta}_{ij}=\begin{cases}\frac{N_j^+\alpha_{ij}-N_{u_1}^+\alpha_{iu_1}\tilde{\beta}_{u_1j}}{N_i^-} & (j\neq u_1)\\ -\frac{N_{u_1}^+\alpha_{iu_1}\tilde{\beta}_{u_1u_1}}{N_i^-} & (j=u_1)\end{cases}. \tag{30}$$

We obtain the Bogoliubov transformation which relates the out-mode operators and the in-mode operators:

$$\begin{pmatrix} (\hat{a}^{\rm in}_{\bar{u}})^\dagger \\ \hat{a}^{\rm in}_{v} \\ \hat{a}^{\rm in}_{u_1} \\ \hat{a}^{\rm in}_{u_2} \end{pmatrix} = \begin{pmatrix} \beta_{\bar{u}\bar{u}} & \beta_{\bar{u}v} & \beta_{\bar{u}u_1} & \beta_{\bar{u}u_2} \\ \beta_{v\bar{u}} & \beta_{uv} & \beta_{vu_1} & \beta_{vu_2} \\ \beta_{u_1\bar{u}} & \beta_{u_1v} & \beta_{u_1u_1} & \beta_{u_1u_2} \\ \beta_{u_2\bar{u}} & \beta_{u_2v} & \beta_{u_2u_1} & \beta_{u_2u_2} \end{pmatrix} \begin{pmatrix} (\hat{a}^{\rm out}_{\bar{u}})^\dagger \\ \hat{a}^{\rm out}_{v} \\ \hat{a}^{\rm out}_{u_1} \\ \hat{a}^{\rm out}_{u_2} \end{pmatrix}, \tag{31}$$

where $\{\beta_{ij}\}$ satisfies the relation $\sum_k \tilde{\beta}_{ik}\beta_{kj} = \delta_{ij}$.

IV. VACUUM STATE

The Bogoliubov transformation involving the $\bar{u}$ mode is given by

$$\hat{a}^{\rm in}_{\bar{u}} = \beta^*_{\bar{u}\bar{u}}\hat{a}^{\rm out}_{\bar{u}} + \beta^*_{\bar{u}v}(\hat{a}^{\rm out}_{v})^\dagger + \beta^*_{\bar{u}u_1}(\hat{a}^{\rm out}_{u_1})^\dagger + \beta^*_{\bar{u}u_2}(\hat{a}^{\rm out}_{u_2})^\dagger, \tag{32}$$

where $|\beta_{\bar{u}\bar{u}}|^2 - |\beta_{\bar{u}v}|^2 - |\beta_{\bar{u}u_1}|^2 - |\beta_{\bar{u}u_2}|^2 = 1$ holds. The equality $\beta_{\bar{u}u_2} = 0$ holds for the subsonic case with the GVH and the trans-sonic case because there exists no u_2 mode in the out-state. The Bogoliubov coefficients related to the $\bar{u}$ mode can be parametrized as

$$\begin{aligned} &\beta_{\bar{u}\bar{u}} = e^{i\phi_1}\cosh r, \quad \beta_{\bar{u}v} = e^{i\phi_2}\sinh r\sin\theta, \\ &\beta_{\bar{u}u_1} = e^{i\phi_3}\sinh r\cos\theta\sin\phi, \quad \beta_{\bar{u}u_2} = e^{i\phi_4}\sinh r\cos\theta\cos\phi, \end{aligned} \tag{33}$$

where $r, \theta, \phi, \phi_1, \phi_2, \phi_3, \phi_4$ are real parameters. r is the squeezing parameter, and as $r \to 0$, the number of created particles decreases. θ represents a ratio of the u mode and the v mode; as $\theta \to 0$, mixing of the u mode and v mode becomes small. The parameter ϕ represents the ratio of the u_1 mode and u_2 mode.

With these parameters, we can characterize the out-vacuum state. Let us define new annihilation operators $\hat{A}_1, \hat{A}_2, \hat{A}_3, \hat{A}_4$ from the in-mode annihilation operators by

$$\hat{A}_1 = \hat{a}^{\rm out}_{\bar{u}}, \tag{34}$$

$$\begin{aligned} \hat{A}_2 = {} & e^{i(\phi_3-\phi_1)}\sin\theta\cos\phi\hat{a}^{\rm out}_{u_1} + e^{i(\phi_4-\phi_1)}\sin\theta\sin\phi\hat{a}^{\rm out}_{u_2} \\ & + e^{i(\phi_2-\phi_1)}\cos\theta\hat{a}^{\rm out}_{v}, \end{aligned} \tag{35}$$

$$\begin{aligned} \hat{A}_3 = {} & -e^{i(\phi_3-\phi_1)}\cos\theta\cos\phi\hat{a}^{\rm out}_{u_1} - e^{i(\phi_4-\phi_1)}\cos\theta\sin\phi\hat{a}^{\rm out}_{u_2} \\ & + e^{i(\phi_2-\phi_1)}\sin\theta\hat{a}^{\rm out}_{v}, \end{aligned} \tag{36}$$

$$\hat{A}_4 = -e^{i(\phi_3-\phi_1)}\sin\phi\hat{a}^{\rm out}_{u_1} + e^{i(\phi_4-\phi_1)}\cos\phi\hat{a}^{\rm out}_{u_2}. \tag{37}$$

These new operators satisfy $[\hat{A}_i, \hat{A}_j] = 0$ and $[\hat{A}_i, \hat{A}^\dagger_j] = \delta_{ij}$. With these new operators, from Eq. (31), annihilation operators of the in-mode can be written as

$$\hat{a}^{\rm in}_{\bar{u}} = e^{i\phi_1}(\cosh r\hat{A}_1 + \sinh r\hat{A}^\dagger_2), \tag{38}$$

$$\begin{aligned} \hat{a}^{\rm in}_{v} = {} & e^{i\phi'_1}\left[\frac{\rho}{\cosh r}(\sinh r\hat{A}^\dagger_1 + \cosh r\hat{A}_2)\right. \\ & \left. + \sqrt{1 - \frac{|\rho|^2}{\cosh^2 r}}(\cos\phi'\hat{A}_3 + \sin\phi'\hat{A}_4)\right], \end{aligned} \tag{39}$$

$$\begin{aligned} \hat{a}^{\rm in}_{u_1} = {} & e^{i\phi'_2}\left[\frac{\rho'}{\cosh r}(\sinh r\hat{A}^\dagger_1 + \cosh r\hat{A}_2)\right. \\ & \left. + \sqrt{1 - \frac{|\rho'|^2}{\cosh^2 r}}(\cos\phi''\hat{A}_3 + \sin\phi''\hat{A}_4)\right], \end{aligned} \tag{40}$$

$$\begin{aligned} \hat{a}^{\rm in}_{u_2} = {} & e^{i\phi'_3}\left[\frac{\rho''}{\cosh r}(\sinh r\hat{A}^\dagger_1 + \cosh r\hat{A}_2)\right. \\ & \left. + \sqrt{1 - \frac{|\rho''|^2}{\cosh^2 r}}(\cos\phi'''\hat{A}_3 + \sin\phi'''\hat{A}_4)\right], \end{aligned} \tag{41}$$

where we introduced new constants $\phi'_1, \phi'_2, \phi'_3, \phi'', \phi'''$, ρ, ρ', ρ'' which are related to the original parameters $\phi_1, \phi_2, \phi_3, \phi_4, \beta_{ij}$. From these relations, the vacuum condition for the in-state yields

$$\begin{aligned} &(\cosh r\hat{A}_1 + \sinh r\hat{A}^\dagger_2)|0_{\rm in}\rangle = 0, \\ &(\sinh r\hat{A}^\dagger_1 + \cosh r\hat{A}_2)|0_{\rm in}\rangle = 0, \end{aligned} \tag{42}$$

$$\hat{A}_3|0_{\rm in}\rangle = 0, \qquad \hat{A}_4|0_{\rm in}\rangle = 0, \tag{43}$$

and the in-vacuum state is written as

$$|0_{\rm in}\rangle = \frac{1}{\cosh r}\sum_{n=0}^{\infty}(-\tanh r)^n|n_{A_1}\rangle|n_{A_2}\rangle|0_{A_3}\rangle|0_{A_4}\rangle. \tag{44}$$

Thus the in-vacuum state is the two mode squeezed state of the A_1 mode and A_2 mode.

To quantify the entanglement structure between modes, we use negativity as the entanglement criterion. See Appendix B for the method to calculate negativity from the Bogolyubov coefficients.

V. RESULTS

Our analysis is performed for the subsonic case and the trans-sonic case. For the subsonic case, there are right-moving modes with low frequency ω in $x < 0$; however, there exists a critical frequency $\omega_{\rm GVH}$ such that there is no right-moving mode with frequencies $\omega > \omega_{\rm GVH}$ in $x < 0$. This means that modes with sufficiently high frequency can feel the effective sonic horizon (GVH) at $x = 0$ even for the subsonic case. For the trans-sonic case, there is no right-moving mode in the supersonic region $x < 0$, and the point $x = 0$ is the sonic horizon.

In our analysis, we adopt two sets of parameters $\{k_0 = 100, V_+ = -0.4, V_- = -0.6\}$ (subsonic case) and $\{k_0 = 100, V_+ = -0.75, V_- = -1.25\}$ (trans-sonic case).

Corresponding to the cutoff wave number k_0, the cutoff frequency ω_c is determined by V_+ and k_0. The value of $\omega_{\rm GVH}$ is given by a point at which the line $\Omega = c_s(k)k$ is tangent to $\Omega = \omega - V_- k$ in the dispersion diagram:

$$\omega_{\rm GVH} = \frac{k_0}{16}\left(3V_- + \sqrt{V_-^2+8}\right) \times \sqrt{8 - 2V_-^2 + 2V_-\sqrt{V_-^2+8}}. \quad (45)$$

The value of ω_c is given by a point at which the line $\Omega = c(k)k$ is tangent to $\Omega = \omega - V_+ k$ in the dispersion diagram:

$$\omega_c = \frac{k_0}{16}\left(3V_+ + \sqrt{V_+^2+8}\right) \times \sqrt{8 - 2V_+^2 + 2V_+\sqrt{V_+^2+8}}. \quad (46)$$

For the subsonic case, $\omega_c/k_0 = 0.240, \omega_{\rm GVH}/k_0 = 0.133$, and $\omega_{\rm GVH}/\omega_c = 0.554$. For the trans-sonic case, $\omega_c/k_0 = 0.0666$.

A. Power spectrum of created particles

The power spectrum of out-going particles (radiations) is represented as

$$f_{u_1}(\omega) = |\beta_{u_1\bar{u}}|^2, \qquad f_{u_2}(\omega) = |\beta_{u_2\bar{u}}|^2,$$
$$f_v(\omega) = |\beta_{v\bar{u}}|^2, \qquad f_{\bar{u}}(\omega) = |\beta_{\bar{u}\,\bar{u}}|^2 - 1. \quad (47)$$

For these power spectrums, we introduce the effective temperature $T_i(\omega)$ by the relation

$$f_i(\omega) = \frac{1}{e^{\omega/T_i(\omega)} - 1}. \quad (48)$$

If the effective temperature is constant with respect to ω in some frequency range, the power spectrum has a Planckian distribution in that frequency range, and radiation cannot be distinguished from the thermal one.

1. Subsonic case

For the subsonic case, the analytical formula of the power spectrum in the low frequency region [15] is

$$|\beta_{u_1\bar{u}}|^2 \approx \frac{\sqrt{1-V_+}(V_+ - V_-)^2}{4(V_+ + 1)^{3/2}(V_- + 1)^2}\frac{\omega}{k_0}, \qquad \omega/k_0 \ll 1. \quad (49)$$

Particle creation in the low frequency region occurs due to the Planckian mode associated with the nonlinear dispersion. Actually for $k_0 \to \infty$ with fixed ω, the created particle number becomes zero. For a high frequency region over $\omega_{\rm GVH}$, particle creation occurs due to the mode conversion associated to the GVH, which is also related to the Planckian mode.

We plot our result of power spectrums in Fig. 4, where frequency is normalized, so the cutoff frequency becomes equal to 1. From ω dependence of the effective temperature (Fig. 5), the thermality of the spectrum is not observed for $\omega < \omega_{\rm GVH}$. In the $\omega \to 0$ limit, the number of u_1 particles becomes zero, but finite numbers of $\bar{u}$ particles and u_2 particles are created, and the numbers of these particles are almost same. However, the behavior of power spectrums for these particles in the higher frequency region is quite different. The number of $\bar{u}$ particles increases with the increase of frequency until the frequency reaches $\omega_{\rm GVH}$, at which point the GVH appears. After the GVH is formed, the number of $u_1, \bar{u}$ particles decreases as frequency increases. The number of u_2 particles decreases with the increase of frequency, and becomes zero after the GVH is formed. The number of v particles increases smoothly across $\omega = \omega_{\rm GVH}$ as frequency increases.

The effective temperature does not become constant in any frequency region (left panel of Fig. 5). This means the power spectrum cannot be regarded as Planckian distribution in any frequency region. If we define the effective temperature by adding a parameter μ_i as

$$f_i(\omega) = \frac{1}{e^{(\omega+\mu_i)/T_i(\omega)} - 1}, \quad (50)$$

the effective temperature becomes constant for $\omega \geq \omega_{\rm GVH}$ and around $\omega \sim \omega_{\rm GVH}$ if we choose an appropriate value of μ_i (right panel of Fig. 5). This implies the power spectrum is indistinguishable from the thermal one with chemical potential μ_i if we observe the emitted particles with frequency around $\omega \sim \omega_{\rm GVH}$.

2. Trans-sonic case

In this case, the power spectrum in the low frequency region [14,15] is

$$|\beta_{u_1\bar{u}}|^2 \approx \frac{(V_+ + 1)^{3/2}(V_- + 1)(V_+ + V_-)}{\sqrt{1-V_+}(-V_- + 1)(V_+ - V_-)}\frac{k_0}{\omega}, \qquad \omega/k_0 \ll 1. \quad (51)$$

Figure 6 shows power spectrums of emitted radiations in this case. In the low frequency region, spectrums of $u_1, \bar{u}$ particles are thermal, and they decrease rapidly near the cutoff frequency ω_c. The number of the v particles shows behavior similar to that for the subsonic case.

Figure 7 shows the behavior of the effective temperature for the u_1 particle. Around $\omega \sim 0$, it becomes constant which reflects the thermal property of emitted radiation.

For the trans-sonic case with $\omega \sim 0$, neglecting the contribution of the v mode, the Bogoliubov coefficients satisfy $|\beta_{u_1u_2}|^2 - |\beta_{u_1\bar{u}}|^2 \approx 1$. These coefficients diverge as $1/\omega$. Using this relation, the power spectrum of the u_1 particle is

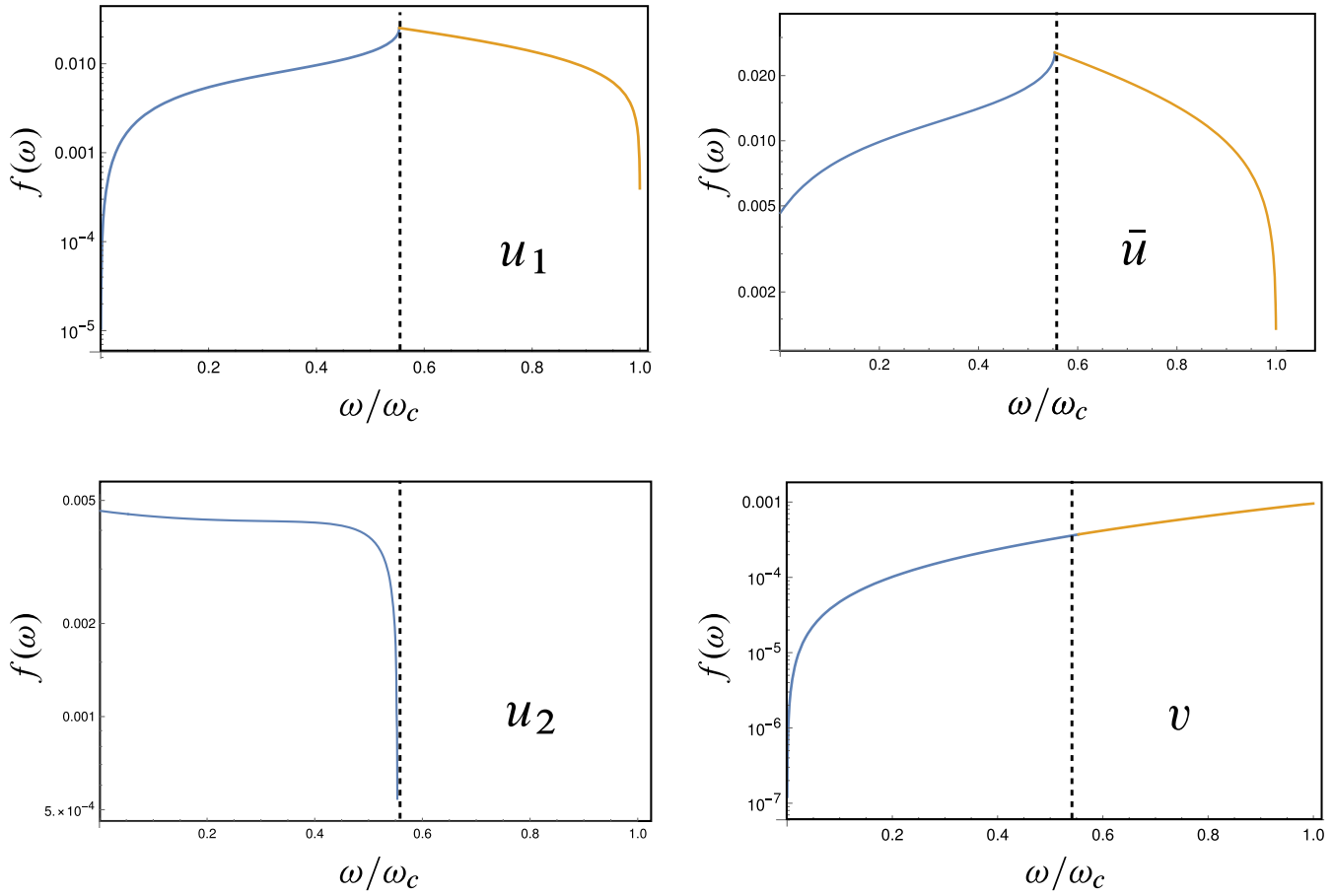

FIG. 4. Power spectrums of created particles for the subsonic case. $\omega_{\mathrm{GVH}}/\omega_c = 0.554$ for the present parameters. Across $\omega = \omega_{\mathrm{GVH}}$, the number of modes changes from four to three, and the spectrums of $u_1, \bar{u}, u_2$ are not smooth at ω_{GVH}.

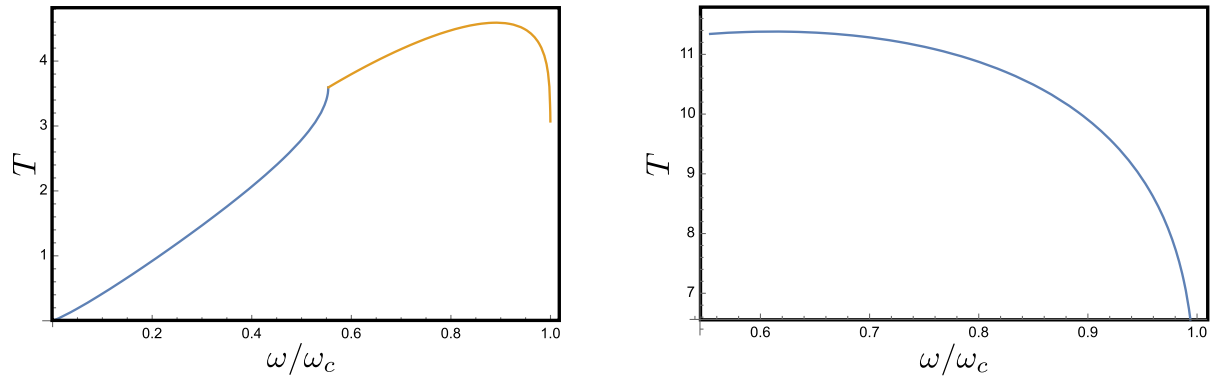

FIG. 5. Left: effective temperature of u_1 particle determined by Eq. (48) for the subsonic case. The effective temperature does not become constant for any frequency region. Right: effective temperature of u_1 particle determined by Eq. (50) for $\omega \geq \omega_{\mathrm{GVH}}$ for the subsonic case. The effective temperature becomes constant around $\omega \sim \omega_{\mathrm{GVH}}$. In this plot, we chose $\mu_i = 1.2\omega_c$.

$$|\beta_{u_1\bar{u}}|^2 \approx \left(\left|\frac{\beta_{u_1u_2}}{\beta_{u_1\bar{u}}}\right|^2 - 1\right)^{-1}. \tag{52}$$

The ratio $|\beta_{u_1u_2}/\beta_{u_1\bar{u}}|$ determines the power spectrum of the u_1 particle. As $\omega \to 0$ the ratio $|\beta_{u_1u_2}/\beta_{u_1\bar{u}}|$ goes to 1 for the trans-sonic case; this behavior of the Bogoliubov coefficients originated from the boundary condition for the decaying wave function in $x < 0$ (see Appendix C for details). The ratio can be approximated as

$$\left|\frac{\beta_{u_1u_2}}{\beta_{u_1\bar{u}}}\right| \simeq 1 + \gamma\omega \approx e^{\gamma\omega}, \tag{53}$$

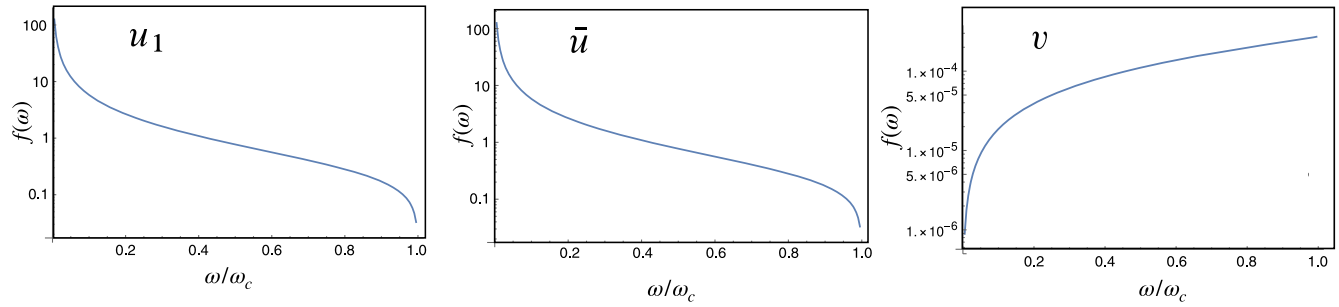

FIG. 6. Power spectrums for the trans-sonic case.

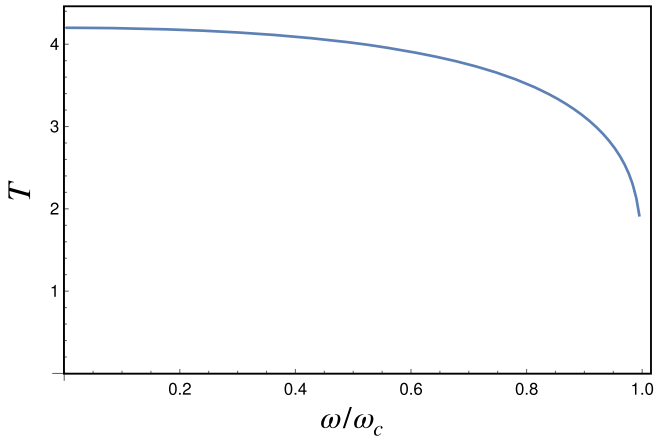

FIG. 7. Effective temperature of the u_1 particle for the trans-sonic case. Around $\omega \sim 0$, the effective temperature becomes constant.

where γ is a factor determined by $V_\pm$. This approximation indicates that the power spectrum of the u_1 particle shows thermal distribution with effective temperature $T = 1/(2\gamma)$ in the low frequency range. Using (51), the temperature is given by

$$T(\omega = 0) = \frac{(V_+ + 1)^{3/2}(V_- + 1)(V_+ + V_-)}{\sqrt{1 - V_+}(-V_- + 1)(V_+ - V_-)} k_0. \tag{54}$$

This formula provides a numerical value of the temperature as $T(\omega = 0) = 4.20$ for present parameters and is consistent with the numerical result (Fig. 7). However, this temperature seems to have nothing to do with the surface gravity of the horizon because it diverges for the step velocity profile, and the thermal property appears due to nonlinear dispersion relation (the Planckian mode). Indeed, the temperature (54) can be regarded as corresponding to the effective surface gravity which is defined by the velocity difference divided by the effective thickness of the sonic horizon determined by the cutoff wave number k_0.

B. Entanglement structure

1. Subsonic case

To analyze entanglement between each particle mode, we calculated parameters r, θ, ϕ introduced in the previous section. These parameters determine components of the covariance matrix for the vacuum state. Figure 8 shows the behavior of these parameters for the sub-sonic case. The squeezing parameter r increases with the increase of frequency until ω_{GVH}, and then decreases with the increase of ω. The mixing parameters θ and ϕ go to zero as $\omega \to 0$, and increase with the increase of ω. Thus from the definition of parameters (33), the u_2 particle (Plankian mode) is mainly created for $\omega \to 0$. As ω increases, the number of u_1 particles increases until ω_{GVH}. For $\omega_{\mathrm{GVH}} < \omega$, as the GVH is formed, the creation of the u_2 particle is shut down, and the u_1 particle and $\bar{u}$ particle mainly contribute as created particles.

Behavior of the entanglement negativity for the subsonic case is shown in Figs. 9–11. Figure 9 is the negativity for bipartitioning of the total pure system [four modes for

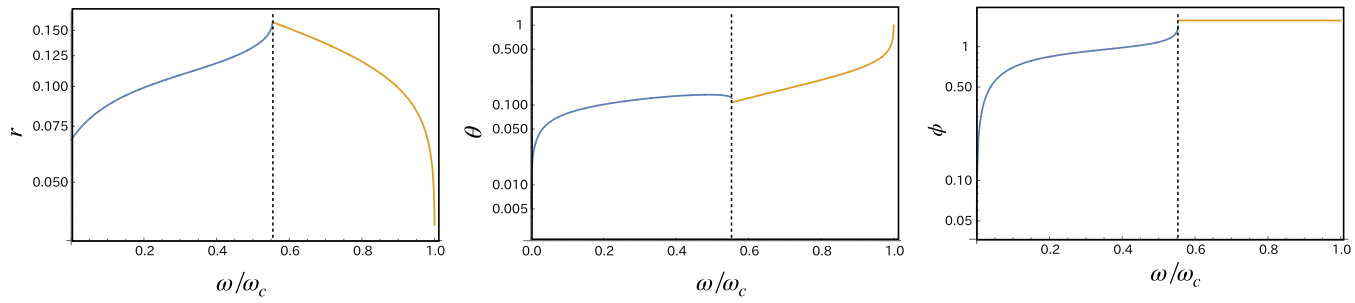

FIG. 8. Behavior of parameters r, θ, ϕ for the subsonic case.

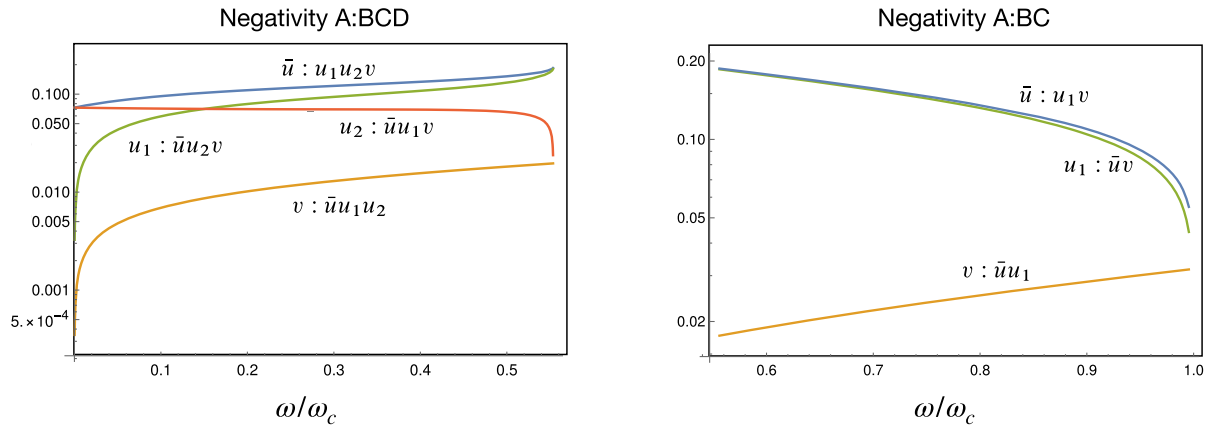

FIG. 9. Negativity for the subsonic case. For low frequency $\omega < \omega_{\mathrm{GVH}}$ (left panel), the number of particle modes is four. For high frequency $\omega_{\mathrm{GVH}} < \omega$ (right panel), the number of particle modes is three.

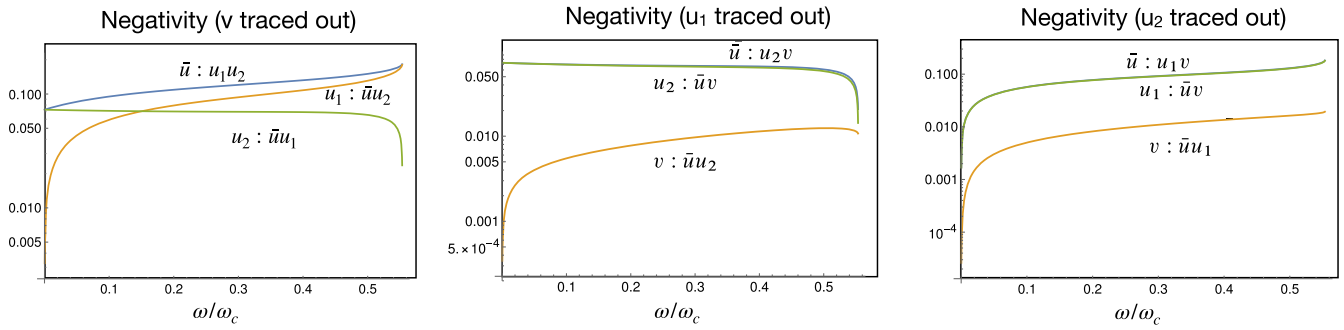

FIG. 10. Negativity of reduced state for the subsonic case in the low frequency region $0 < \omega < \omega_{\mathrm{GVH}}$.

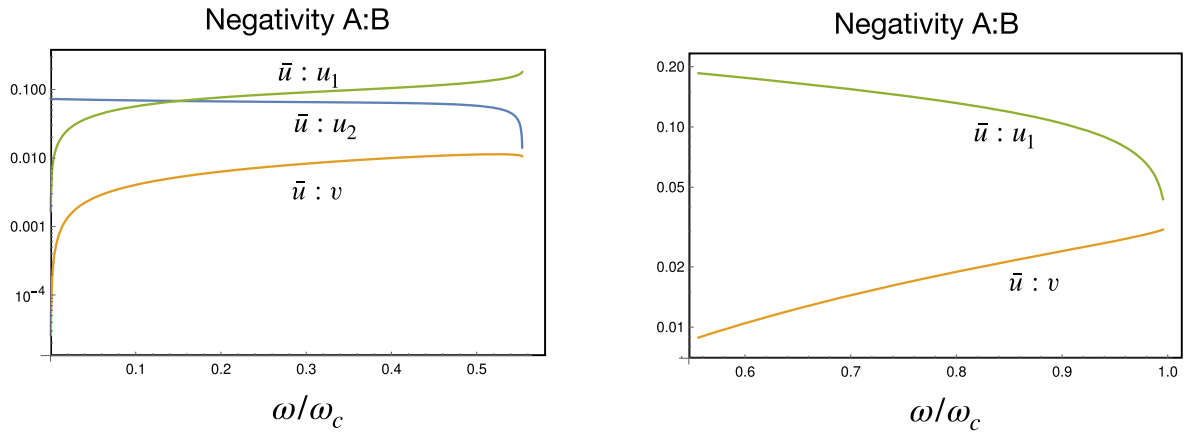

FIG. 11. Negativity of reduced two mode state for the subsonic case.

$\omega < \omega_{\mathrm{GVH}}$ (left panel) and three modes for $\omega_{\mathrm{GVH}} < \omega$ (right panel)]. For $\omega < \omega_{\mathrm{GVH}}$, entanglement between u_1, v particles and other particles goes to zero as $\omega \to 0$. This decrease of entanglement corresponds to the decrease of the created number of u_1 particles and v particles. Entanglement between $\bar{u}, v, u_1$ particles and other particles increases with the increase of ω, whereas entanglement between the u_2 particle and other particles decreases. For $\omega_{\mathrm{GVH}} < \omega$ where the GVH exists, the u_2 particle disappears, and the total number of modes becomes three. Entanglement between $\bar{u}, u_1$ particles and other particles decreases, and entanglement between the v particle and other particles increases with the increase of ω.

In the limit of $\omega \to 0$, u_1 and v modes are separable from the three other modes, and the u_2 and $\bar{u}$ mode forms an entangled pair. With the increase of frequency, entanglement

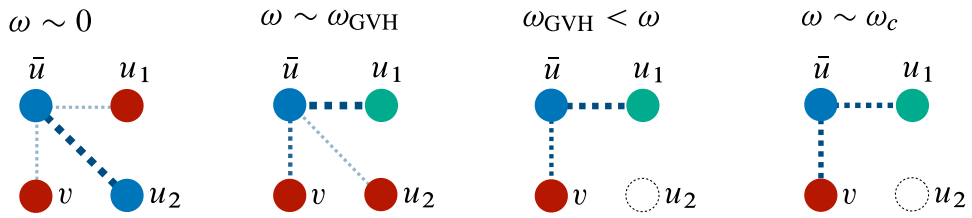

FIG. 12. Schematic pictures of entanglement structure for the subsonic case. Red disks represent non-Planckian modes, blue disks represent the Planckian mode, and green disks represent sub-Planckian modes. For low frequency, entanglement of the system is shared mainly by $\bar{u} - u_2$ pair. For $\omega \sim \omega_{\mathrm{GVH}}$, entanglement of the system is shared mainly by $\bar{u} - u_1$ pair.

between u_1 and $\bar{u}$ modes, and entanglement between v and $\bar{u}$ modes become larger. And near the frequency ω_{GVH}, entanglement between the u_1 and $\bar{u}$ modes becomes the main contribution to entanglement of the four modes system. For $\omega > \omega_{\mathrm{GVH}}$, entanglement between the u_1 and $\bar{u}$ modes starts to decrease, whereas entanglement between the v and $\bar{u}$ modes keeps increasing, and their amount becomes comparable near the cutoff frequency ω_c. We present schematic pictures of the entanglement structure in Fig. 12.

For $\omega \sim 0$, non-Planckian modes u_1, v cannot entangle with Planckian modes $u_2, \bar{u}$. With the increase of frequency, the non-Planckian mode u_1 becomes the sub-Planckian mode, and $\bar{u}$ and u_1 are entangled. This is the reason why entanglement between u_1 and other modes gets larger with the increase of frequency in the low frequency region.

Now let us comment on the property of the radiation for $\omega_{\mathrm{GVH}} < \omega$ where the GVH exists. For models with slowly varying velocity profiles, in the vicinity of the GVH, the wave number corresponding to emitted particles is expressed as

$$k(x) \approx \frac{\omega}{\kappa(x - x_0) + \omega/k(x_0) + k(x_0)\partial c_s/\partial k|_{k(x_0)}}, \quad (55)$$

where x_0 is the location of the GVH, κ is the first derivative of the velocity profile at the GVH, and $k(x_0)$ is the wave number at the GVH (see Appendix D for the derivation of this formula). This x dependence of the wave number is the same as the behavior of the wave number of the trans-sonic case if we regard the location $x^* = x_0 - (\omega/k(x_0) - k(x_0)\partial c_s/\partial k|_{k(x_0)})/\kappa$ as the sonic horizon hidden inside the group velocity horizon. We remark that Eq. (55) can approximate the behavior only outside the group velocity horizon. If we construct the global solution which can be connected to the u_1 out mode in $x \to \infty$, it is a decaying function inside the group velocity horizon, and no singular behavior as expressed by Eq. (55) appears in reality. We also remark that x^* corresponds to the real sonic horizon when the sonic horizon exists. Since the behavior of the wave number of the Hawking mode is not distinguishable from that of the trans-sonic case, we can use the method of Laplace transformation and the saddle point approximation well discussed in the previous research [9,10,23], and we obtain thermal behavior of the radiation. The bipartite entanglement for $\omega_{\mathrm{GVH}} < \omega$ decreases with the increase of ω, which is the same behavior for the trans-sonic case and related to the thermal property of radiations. These considerations suggest that the mechanism of the particle creation for $\omega_{\mathrm{GVH}} < \omega$ is analogous to that of the trans-sonic one although the analogous spacetime does not have the sonic horizon.

2. Transsonic case

Figure 13 shows the ω dependence of parameters r, θ, ϕ, and Fig. 14 shows negativity for the trans-sonic case. Entanglement between $\bar{u}, u_1$ modes and other modes decreases with the increase of ω, and entanglement between the v mode and other modes also increases with the increase of ω. This behavior is consistent with that of

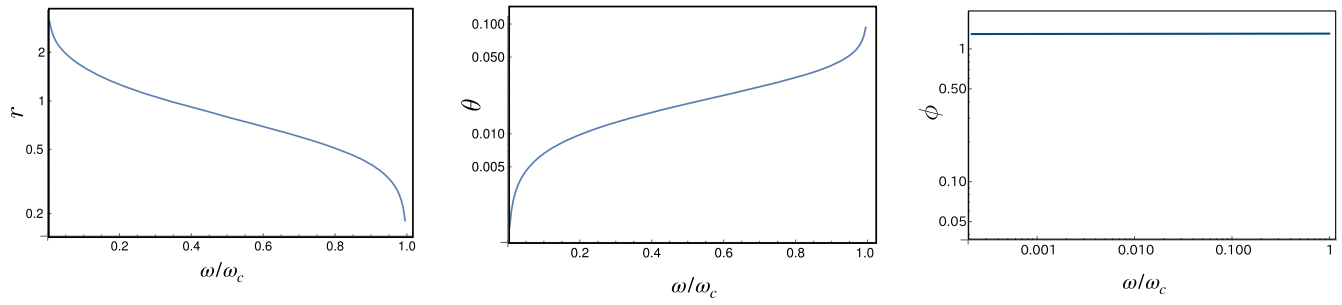

FIG. 13. Frequency dependence of parameters r, θ, ϕ for the trans-sonic case.

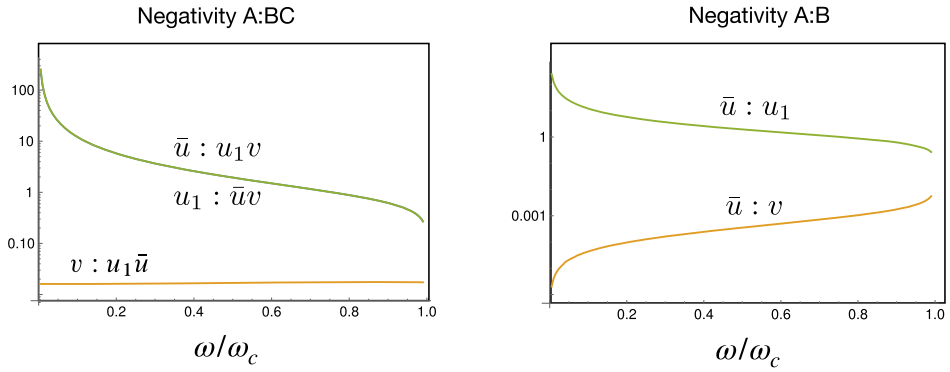

FIG. 14. Behavior of negativity for the trans-sonic case.

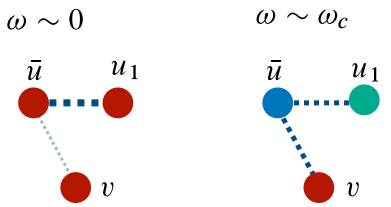

FIG. 15. Schematic pictures of entanglement structure for the trans-sonic case. Red disks represent non-Planckian modes, blue disks represent Planckian modes, and green disks represent sub-Planckian modes. For low frequency, entanglement of the system is shared mainly by the $\bar{u}$-u_1 pair.

the power spectrum; with the increase of entanglement, the number of created particles increases.

For the $\omega \to 0$ limit, the v mode becomes approximately separable from other modes, and u_1 and $\bar{u}$ are entangled. With the increase of ω, entanglement between the u_1 and $\bar{u}$ modes decreases, and entanglement between the v and $\bar{u}$ modes increases. And the amount of these entanglements becomes comparable near the cutoff frequency ω_c. This behavior is the same as that observed in our previous study for the trans-sonic flow with finite surface gravity at the sonic horizon [20]. A schematic structure of entanglement for the trans-sonic case is shown in Fig. 15.

VI. CONCLUSION

We have calculated the power spectrum and entanglement of the scalar field modes in the dispersive media with a step velocity profile. For the trans-sonic case, we have obtained the similar result as [20], but the temperature of the radiation is given by Eq. (54), which is not equal to the derivative of the fluid velocity at the sonic horizon. For the subsonic case, the situation is completely different. Entanglement between the u_1 mode and $\bar{u}$ mode, and the power spectrum of the created u_1 particle increases with frequency ω until the frequency reaches ω_{GVH} where the GVH appears. The power spectrum becomes a decreasing function of frequency for $\omega_{\mathrm{GVH}} < \omega$. For the dispersive model investigated in this paper, the power spectrum of the u_1 mode for the subsonic case and for the trans-sonic case has a similar behavior in the high frequency region. Concerning entanglement structure, we found that Planckian modes cannot entangle with non-Planckian modes (see Figs. 12 and 15); for the subsonic case, in the low frequency limit, the u_1 mode and v mode are non-Planckian modes, and the $\bar{u}$ mode and u_2 mode are Planckian modes. Entanglement of the system is shared only between the u_2 mode and $\bar{u}$ mode, and the u_1 particle is not created. With the increase of frequency, the u_1 mode becomes a sub-Planckian mode and the u_1 particle can be created. For the trans-sonic case, all of the modes are sub-Planckian modes in the low frequency limit, and the u_1 mode and $\bar{u}$ mode can entangle. From the viewpoint of entanglement, the sonic horizon and the group velocity horizon are indistinguishable; they both lead to the dominant entanglement between the u_1 mode and $\bar{u}$ mode. In this paper, we choose a steplike velocity profile for the simplicity. However, the results remain valid even in the more realistic case where the velocity profile is not exactly steplike, but rather smoothed. This is because the value of the surface gravity is unimportant for the small cutoff case $T_H > \omega_{\mathrm{cutoff}}$ as we have shown in our previous paper [20]. While we did not discuss these issues in this paper, we are interested in the following topics: the first one is how the cutoff scale affects the total energy and the total entanglement of modes. We do not understand how the total energy of modes and entanglement is shared between modes with nonlinear dispersions. The second one is the behavior of two point correlation functions. Two point correlation functions for analog black holes are investigated in [24–27]. It may be interesting to evaluate them for the subsonic case without a sonic horizon. The third one is the dependence of dispersion relation on particle creations and entanglement. We considered the subluminal dispersion in this paper, but for the superluminal dispersion, the number of the negative norm modes is different, and we expect a different entanglement structure. The final one is the case with the time dependent velocity profile. The dispersion relation is modified due to the inclusion of an additional self-interaction term in the Lagrangian. However,

we need to consider the loop correction when we construct the out vacuum state [28–31] for the dynamical cases. The behavior of the number density or the entanglement structure for such cases would not exhibit the thermal property even for the small frequency. These problems are left for our future research.

ACKNOWLEDGMENTS

Y. N. was supported in part by JSPS KAKENHI Grant No. 19K03866.

APPENDIX A: CALCULATION OF THE BOGOLIUBOV COEFFICIENTS

By specifying a mode in $x<0$, it is possible to obtain a wave function which satisfies a given boundary condition in $x<0$. Schematic diagrams describing four possible different boundary conditions in the $x<0$ region are shown in Fig. 16.

For the plane wave $\exp(ik_i^- x)$ in $x<0$ with a real wave number k_i^-, we can define the normalized mode function $\phi_i^{\mathrm{in/out}}(x)=\exp(ik_i^{\mathrm{in/out}}x)/N_i^{\pm}$ with

$$N_i^{\pm}=\sqrt{4\pi c_s(k_i^{\pm})k_i^{\pm}v_g(k_i^{\pm})},\qquad v_g=\left(\frac{dk}{d\omega}\right)^{-1}. \tag{A1}$$

We put labels "±" and "in/out" depending on the asymptotic regions and the sign of the group velocity. If all modes are normalizable (i.e., all solutions of the dispersion relation are real), plane wave solutions with specified boundary conditions are given as follows:

$$\text{(a) } \phi(x)=\begin{cases} N_{u_1}^-\phi_{u_1}^{\mathrm{in}} & (x<0)\\ N_{u_1}^+\alpha_{u_1u_1}\phi_{u_1}^{\mathrm{out}}+N_{u_2}^+\alpha_{u_1u_2}\phi_{u_2}^{\mathrm{in}}+N_{\bar u}^+\alpha_{u_1\bar u}\phi_{\bar u}^{\mathrm{in}}+N_v^+\alpha_{u_1v}\phi_v^{\mathrm{in}} & (x>0)\end{cases} \tag{A2}$$

$$\text{(b) } \phi(x)=\begin{cases} N_{u_2}^-\phi_{u_2}^{\mathrm{out}} & (x<0)\\ N_{u_1}^+\alpha_{u_2u_1}\phi_{u_1}^{\mathrm{out}}+N_{u_2}^+\alpha_{u_2u_2}\phi_{u_2}^{\mathrm{in}}+N_{\bar u}^+\alpha_{u_2\bar u}\phi_{\bar u}^{\mathrm{in}}+N_v^+\alpha_{u_2v}\phi_v^{\mathrm{in}} & (x>0)\end{cases} \tag{A3}$$

$$\text{(c) } \phi(x)=\begin{cases} N_{\bar u}^-\phi_{\bar u}^{\mathrm{out}} & (x<0)\\ N_{u_1}^+\alpha_{\bar u u_1}\phi_{u_1}^{\mathrm{out}}+N_{u_2}^+\alpha_{\bar u u_2}\phi_{u_2}^{\mathrm{in}}+N_{\bar u}^+\alpha_{\bar u\bar u}\phi_{\bar u}^{\mathrm{in}}+N_v^+\alpha_{u_1v}\phi_v^{\mathrm{in}} & (x>0)\end{cases} \tag{A4}$$

$$\text{(d) } \phi(x)=\begin{cases} N_{u_1}^-\phi_{u_1}^{\mathrm{out}} & (x<0)\\ N_{u_1}^+\alpha_{vu_1}\phi_{u_1}^{\mathrm{out}}+N_{u_2}^+\alpha_{vu_2}\phi_{u_2}^{\mathrm{in}}+N_{\bar u}^+\alpha_{v\bar u}\phi_{\bar u}^{\mathrm{in}}+N_v^+\alpha_{vv}\phi_v^{\mathrm{in}} & (x>0).\end{cases} \tag{A5}$$

Even if there exist unnormalizable modes, the logic is essentially the same, but we have to treat the norm of modes more carefully. From Eqs. (A2)–(A5), we can read off relations between the in-mode functions and the out-mode functions. For example, let us consider Eq. (A2). In the asymptotic out region, the wave function is expressed as $\phi(x)=N_{u_1}^+\alpha_{u_1u_1}\phi_{u_1}^{\mathrm{out}}$; thus this mode defines the out-vacuum state. In the asymptotic in region, the wave function is expressed as the superposition of plane waves

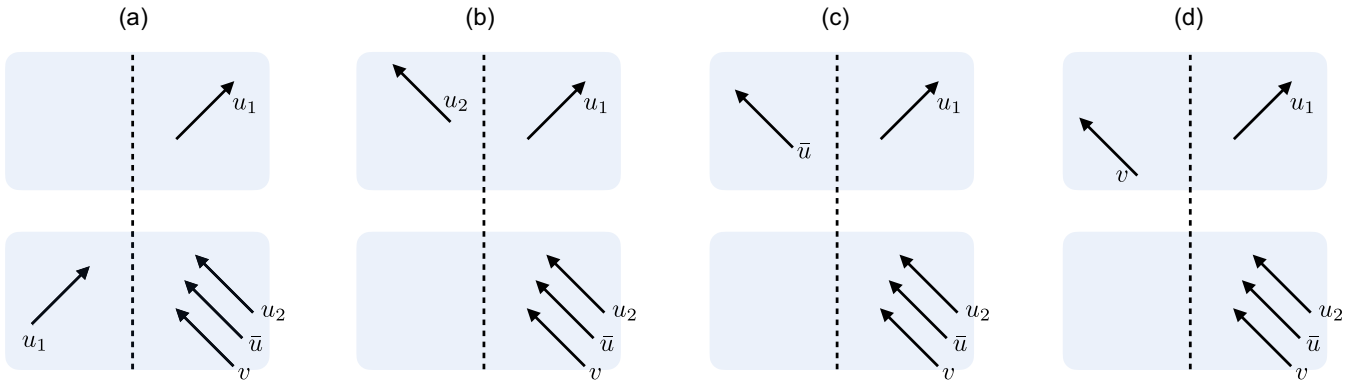

FIG. 16. Four different boundary conditions in $x<0$ for the wave equation (19) to determine the Bogoliubov coefficients. (a) Boundary condition with $\phi^-(x)=\phi_{u_1}^{\mathrm{in}}$. For the subsonic case with $\omega_{\mathrm{GVH}}<\omega$ or the trans-sonic case, the mode u_1 becomes the decaying mode. (b) Boundary condition with $\phi^-(x)=\phi_{u_2}^{\mathrm{out}}$. (c) Boundary condition with $\phi^-(x)=\phi_{\bar u}^{\mathrm{out}}$. (d) Boundary condition with $\phi^-(x)=\phi_v^{\mathrm{out}}$.

$$\phi(x) = N^-_{u_1}\phi^{\rm in}_{u_1} + N^+_{u_2}\alpha_{u_1u_2}\phi^{\rm in}_{u_2} + N^+_{\bar{u}}\alpha_{u_1\bar{u}}\phi^{\rm in}_{\bar{u}} + N^+_v\alpha_{u_1v}\phi^{\rm in}_v. \tag{A6}$$

Therefore, we obtain the following in-out relation

$$N^+_{u_1}\alpha_{u_1u_1}\phi^{\rm out}_{u_1} = N^-_{u_1}\phi^{\rm in}_{u_1} + N^+_{u_2}\alpha_{u_1u_2}\phi^{\rm in}_{u_2} + N^+_{\bar{u}}\alpha_{u_1\bar{u}}\phi^{\rm in}_{\bar{u}} + N^+_v\alpha_{u_1v}\phi^{\rm in}_v. \tag{A7}$$

Repeating the same procedure for the three other boundary conditions, we obtain three other in-out relations:

$$N^-_{u_2}\phi^{\rm out}_{u_2} + N^+_{u_1}\alpha_{u_2u_2}\phi^{\rm out}_{u_1} = N^+_{u_2}\alpha_{u_2u_2}\phi^{\rm in}_{u_2} + N^+_{\bar{u}}\alpha_{u_2\bar{u}}\phi^{\rm in}_{\bar{u}} + N^+_v\alpha_{u_2v}\phi^{\rm in}_v, \tag{A8}$$

$$N^-_{\bar{u}}\phi^{\rm out}_{\bar{u}} + N^+_{u_1}\alpha_{\bar{u}u_1}\phi^{\rm out}_{u_1} = N^+_{u_2}\alpha_{\bar{u}u_2}\phi^{\rm in}_{u_2} + N^+_{\bar{u}}\alpha_{\bar{u}\,\bar{u}}\phi^{\rm in}_{\bar{u}} + N^+_v\alpha_{u_1v}\phi^{\rm in}_v, \tag{A9}$$

$$N^-_{u_1}\phi^{\rm out}_{u_1} + N^+_{u_1}\alpha_{vu_1}\phi^{\rm out}_{u_1} = N_{u_2}\alpha_{vu_2}\phi^{\rm in}_{u_2} + N^+_{\bar{u}}\alpha_{v\bar{u}}\phi^{\rm in}_{\bar{u}} + N^+_v\alpha_{vv}\phi^{\rm in}_v. \tag{A10}$$

By taking the Klein-Gordon inner product of both sides with the field operator $\hat{\phi}$ both sides, from Eq. (18), we obtain the transformation between the in-mode operators and the out-mode operators [Eqs. (28)–(30)]. This transformation is the Bogoliubov transformation, and the transformation is determined by 4×4 Bogoliubov coefficients.

APPENDIX B: ENTANGLEMENT NEGATIVITY

To quantify entanglement between each mode using the negativity, we introduce canonical variables $\hat{X}_i, \hat{P}_i$ by

$$\hat{X}_i = \frac{\hat{a}^{\rm in}_i + (\hat{a}^{\rm in}_i)^\dagger}{\sqrt{2}}, \quad \hat{P}_i = \frac{\hat{a}^{\rm in}_i - (\hat{a}^{\rm in}_i)^\dagger}{i\sqrt{2}}, \quad [\hat{X}_i, \hat{P}_j] = i\delta_{ij}. \tag{B1}$$

Then the wave function of the in-vacuum state is given as

$$\psi_0(X_1, X_2, X_3, X_4) = \langle X_1, X_2, X_3, X_4 | 0_{\rm in}\rangle = \frac{1}{\pi}\exp\left(-\frac{X_1^2 + X_2^2 + X_3^2 + X_4^2}{2}\right). \tag{B2}$$

The Wigner function of this wave function is defined by

$$W(\boldsymbol{X}, \boldsymbol{P}) := \frac{1}{(2\pi)^4}\int d^4\boldsymbol{Y} e^{i\boldsymbol{P}\cdot\boldsymbol{Y}}\psi_0\left(\boldsymbol{X} - \frac{\boldsymbol{Y}}{2}\right)\psi_0^*\left(\boldsymbol{X} + \frac{\boldsymbol{Y}}{2}\right) = \frac{1}{\pi^3}\exp(-\boldsymbol{X}^2 - \boldsymbol{P}^2). \tag{B3}$$

Introducing a vector with canonical variables $\hat{\boldsymbol{\xi}} = (\hat{X}_1, \hat{P}_1, \hat{X}_2, \hat{P}_2, \hat{X}_3, \hat{P}_3, \hat{X}_4, \hat{P}_4)^T$, the covariance matrix is defined by

$$V_{ij} := \left\langle \frac{\hat{\xi}_i\hat{\xi}_j + \hat{\xi}_j\hat{\xi}_i}{2}\right\rangle = \int d^8\boldsymbol{\xi}\xi_i\xi_j W(\boldsymbol{\xi}), \tag{B4}$$

and for the wave function Eq. (B2), $V_{ij} = \delta_{ij}/2$. Since the Bogoliubov transformation preserves commutation relations of creation and annihilation operators, it also keeps commutation relations between canonical variables defined in terms of creation and annihilation operators.

Now we introduce canonical variables for the out modes as

$$\hat{x}_i = \frac{\hat{a}^{\rm out}_i + (\hat{a}^{\rm out}_i)^\dagger}{\sqrt{2}}, \qquad \hat{p}_i = \frac{\hat{a}^{\rm out}_i - (\hat{a}^{\rm out}_i)^\dagger}{i\sqrt{2}},$$

and introduce a vector with canonical variables for the in mode as $\hat{\boldsymbol{\xi}}' = (\hat{x}_1, \hat{p}_1, \hat{x}_2, \hat{p}_2, \hat{x}_3, \hat{p}_3, \hat{x}_4, \hat{p}_4)^T$. The relation between in and out canonical variables is given by

$$\hat{\xi}_i = \sum_j S_i{}^j\hat{\xi}'_j \tag{B5}$$

where

$$S = \begin{pmatrix}
{\rm Re}[\beta_{11}] & {\rm Im}[\beta_{11}] & {\rm Re}[\beta_{12}] & -{\rm Im}[\beta_{12}] & {\rm Re}[\beta_{13}] & -{\rm Im}[\beta_{13}] & {\rm Re}[\beta_{14}] & -{\rm Im}[\beta_{14}] \\
{\rm Im}[\beta_{11}] & {\rm Re}[\beta_{11}] & {\rm Im}[\beta_{12}] & -{\rm Re}[\beta_{12}] & {\rm Im}[\beta_{13}] & -{\rm Re}[\beta_{13}] & {\rm Im}[\beta_{14}] & -{\rm Re}[\beta_{14}] \\
{\rm Re}[\beta_{21}] & {\rm Im}[\beta_{21}] & {\rm Re}[\beta_{22}] & -{\rm Im}[\beta_{22}] & {\rm Re}[\beta_{23}] & -{\rm Im}[\beta_{23}] & {\rm Re}[\beta_{24}] & -{\rm Im}[\beta_{24}] \\
{\rm Im}[\beta_{21}] & {\rm Re}[\beta_{21}] & {\rm Im}[\beta_{22}] & {\rm Re}[\beta_{22}] & {\rm Im}[\beta_{23}] & {\rm Re}[\beta_{23}] & {\rm Im}[\beta_{24}] & {\rm Re}[\beta_{24}] \\
{\rm Re}[\beta_{31}] & {\rm Im}[\beta_{31}] & {\rm Re}[\beta_{32}] & -{\rm Im}[\beta_{32}] & {\rm Re}[\beta_{33}] & -{\rm Im}[\beta_{33}] & {\rm Re}[\beta_{34}] & -{\rm Im}[\beta_{34}] \\
{\rm Im}[\beta_{31}] & -{\rm Re}[\beta_{31}] & {\rm Im}[\beta_{32}] & {\rm Re}[\beta_{32}] & {\rm Im}[\beta_{33}] & {\rm Re}[\beta_{33}] & {\rm Im}[\beta_{34}] & {\rm Re}[\beta_{34}] \\
{\rm Re}[\beta_{41}] & {\rm Im}[\beta_{41}] & {\rm Re}[\beta_{42}] & -{\rm Im}[\beta_{42}] & {\rm Re}[\beta_{43}] & -{\rm Im}[\beta_{43}] & {\rm Re}[\beta_{44}] & -{\rm Im}[\beta_{44}] \\
{\rm Im}[\beta_{41}] & -{\rm Re}[\beta_{41}] & {\rm Im}[\beta_{42}] & {\rm Re}[\beta_{42}] & {\rm Im}[\beta_{43}] & {\rm Re}[\beta_{43}] & {\rm Im}[\beta_{44}] & {\rm Re}[\beta_{44}]
\end{pmatrix} \tag{B6}$$

with the subscript of β_{ij} representing $1,2,3,4=\bar{u}, v, u_1, u_2$. Since this transformation keeps canonical commutation relations, the matrix S satisfies

$$S\Omega S^T=\Omega, \qquad \Omega=\bigoplus_{i=1}^{4}\begin{pmatrix}0 & 1\\ -1 & 0\end{pmatrix}.$$

From $|\det S|=1$, the relation between the in-mode covariance matrix V and the out-mode covariance matrix V' is derived as

$$V_{ij}=\int d^8\boldsymbol{\xi}\xi_i\xi_j W(\xi)=\sum_{k,l}\int d^8\boldsymbol{\xi}' S_i{}^k S_j{}^l \xi'_k\xi'_l W(S(\boldsymbol{\xi}'))$$
$$=(SV'S^T)_{ij}, \tag{B7}$$

where $W(S(\boldsymbol{\xi}'))=W'(\boldsymbol{\xi}')$ is the Wigner function for $\boldsymbol{\xi}'$. Thus the covariance matrix for the out mode can be written as

$$V'=S^{-1}V(S^T)^{-1}=\begin{pmatrix}V_1 & V_2 & V_3 & V_4\\ * & V_5 & V_6 & V_7\\ * & * & V_8 & V_9\\ * & * & * & V_{10}\end{pmatrix}, \tag{B8}$$

where $V_j, j=1,\ldots,10$ denotes 2×2 submatrices of 8×8 covariance matrix V'. For the Gaussian state considered here, it is easy to obtain the covariance matrix for the reduced three mode state by simply integrating out one mode:

$$\tilde{V}_{ij}=\int d^6\boldsymbol{\xi}\xi_i\xi_j\tilde{W}(\boldsymbol{\xi})=\int d^6\boldsymbol{\xi}\xi_i\xi_j\left(\int d^2\boldsymbol{\xi}W(\boldsymbol{\xi})\right)=V_{ij},$$

where $\tilde{W}(\boldsymbol{\xi})$ is the Wigner function for reduced state, and $\tilde{V}_{ij}$ is the covariance matrix of the reduced state. A similar argument can be applied to the covariance matrix of a two mode state. Using the covariance matrix, it is possible to evaluate entanglement negativity which quantifies bipartite entanglement for a given bipartition of the total system (see Appendix B for its definition).

Entanglement of the in-vacuum state is evaluated using the positive partial transpose (PPT) criterion for continuous variable [32–34]. The PPT criterion states that if a partially transposed density matrix has negative eigenvalues, the bipartite state is entangled. For bosonic systems, we can rewrite the PPT criterion in terms of a covariance matrix. From positive definiteness of the density matrix and the uncertainty relation, the covariance matrix which represents a physical state should satisfy

$$V+\frac{i}{2}\Omega\geq 0, \tag{B9}$$

where the inequality of the matrix stands for positive definiteness of the matrix [35]. With this property of a physical density matrix, the PPT criterion is equivalent to the following statement: If the state is separable, the covariance matrix $\tilde{V}$ with the partially transposed density matrix satisfies

$$\tilde{V}+\frac{i}{2}\Omega\geq 0. \tag{B10}$$

The covariance matrix $\tilde{V}$ is easily calculated by inverting the sign of the momentum $p_i\to -p_i$, which corresponds to the partial transposition of a mode [34]. By diagonalization of $\tilde{V}$ using a symplectic matrix S_d,

$$\tilde{V}+\frac{i}{2}\Omega=S_d^T\left(\bigoplus_i\begin{pmatrix}\kappa_i & i/2\\ -i/2 & \kappa_i\end{pmatrix}\right)S_d, \tag{B11}$$

where $\{\kappa_i\}$ are symplectic eigenvalues of $\tilde{V}$. If all of the symplectic eigenvalues are greater than $1/2$, $\tilde{V}+(i/2)\Omega$ is positive definite. To quantify entanglement, the negativity is defined by

$$N=\frac{1}{2}\max\left[\left(\prod_{\kappa_i<1/2}\frac{1}{2\kappa_i}\right)-1,0\right], \tag{B12}$$

and the logarithmic negativity $L_N:=\log(2N+1)$. If $N>0$ or equivalently $L_N>0$ holds when the bipartite state is entangled. Logarithmic negativity is entanglement monotone (does not increase under the Local Operation and Classical Communication) and additive; thus logarithmic negativity can be used as an entanglement measure [36,37].

APPENDIX C: POWER SPECTRUM IN LOW FREQUENCY REGION

For the trans-sonic case, we expand the Bogoliubov coefficients as a power series of ω by comparing the same order terms in both sides of the matching formula. For simplicity, we neglect the uv mixing. The linear combination of the u_1 mode, u_2 mode, and $\bar{u}$ mode is chosen so that it decays exponentially as $x\to-\infty$. We consider wave functions $A\exp\{ik^-_{\rm decay}x\}$ for $x<0$ and $\exp\{ik^+_{u_1}x\}+B\exp\{ik^+_{u_2}x\}+C\exp\{ik^+_{\bar{u}}x\}$ for $x>0$, and match them at $x=0$. The matching formula corresponding to Eq. (21) is written as

$$A=1+B+C, \qquad Ak^-_{\rm decay}=k^+_{u_1}+Bk^+_{u_2}+Ck^+_{\bar{u}},$$
$$A(k^-_{\rm decay})^2=(k^+_{u_1})^2+B(k^+_{u_2})^2+C(k^+_{\bar{u}})^2. \tag{C1}$$

We expand A, B, C in the power of ω as

$$A=A^{(0)}+A^{(1)}\omega+\cdots,$$
$$B=B^{(0)}+B^{(1)}\omega+\cdots,$$
$$C=C^{(0)}+C^{(1)}\omega+\cdots. \tag{C2}$$

We substitute Eq. (C2) into Eq. (C1), and equate terms with the same powers of ω. Wave numbers $k^-_{\rm decay}, k^+_{u_1}, k^+_{u_2}, k^+_{\bar{u}}$ are determined as solutions of the dispersion relation, Eq. (4), as

$$
\begin{aligned}
k^{-}_{\mathrm{decay}} &= ik_0\sqrt{V_-^2-1}+\left(\frac{d\Omega}{dk}\right)^{-1}\omega+\cdots,\\
k^{+}_{u_2} &= k_0\sqrt{1-V_+^2}+\left(\frac{d\Omega}{dk}\right)^{-1}\omega+\cdots,\\
k^{+}_{\bar{u}} &= k_0\sqrt{1-V_+^2}+\left(\frac{d\Omega}{dk}\right)^{-1}\omega\cdots,\\
k^{+}_{u_1} &= \frac{\omega}{1-V_+}.
\end{aligned}
$$

By substituting these expressions into Eq. (C1), we obtain coefficients of the wave function in the lowest order of ω as

$$
\begin{aligned}
A^{(0)} &= 1-\frac{V_-^2-1}{V_-^2-V_+^2},\\
B^{(0)} &= -\frac{1}{2}\left(\frac{V_-^2-1}{V_-^2-V_+^2}-i\sqrt{\frac{V_-^2-1}{1-V_+^2}}\left(1+\frac{V_-^2-1}{V_-^2-V_+^2}\right)\right),\\
C^{(0)} &= -\frac{1}{2}\left(\frac{V_-^2-1}{V_-^2-V_+^2}+i\sqrt{\frac{V_-^2-1}{1-V_+^2}}\left(1+\frac{V_-^2-1}{V_-^2-V_+^2}\right)\right).
\end{aligned}
\tag{C3}
$$

In the zeroth order of ω, $N^{+}_{u_2}=N^{+}_{\bar{u}}$, $|\alpha_{u_1u_2}/\alpha_{u_1\bar{u}}|=|\beta_{u_1u_2}/\beta_{u_1\bar{u}}|=|B^{(0)}/C^{(0)}|=1$ holds. We leave some comments for the subsonic case. Most of the calculations are essentially the same with the trans-sonic case but we need to connect the Hawking mode with the plane wave mode $k^{-}_{u_1}$ instead of the decaying mode. The zeroth order coefficients can be represented by Eq. (C3), but the ratio $|\alpha_{u_1u_2}/\alpha_{u_1\bar{u}}|=|\beta_{u_1u_2}/\beta_{u_1\bar{u}}|=|B^{(0)}/C^{(0)}|$ is not equal to unity since the factor $i\sqrt{V_-^2-1}$ is not purely imaginary. This difference leads to the different behaviors of the power spectrum for the subsonic case and transonic case in the low frequency region.

APPENDIX D: WKB SOLUTIONS FOR SLOWLY VARYING CASE WITH GROUP VELOCITY HORIZON

In this Appendix, let us consider the behavior of the WKB solution in the vicinity of the group velocity horizon. If the velocity profile and the wave number $k(x)$ are the slowly varying function of x, the dispersion relation is given by

$$(\omega-v(x)k)^2=c_s^2(k)k^2. \tag{D1}$$

Since the group velocity horizon is a point where the right-moving mode and left-moving mode in $x>0$ merge due to the subluminal dispersion, the condition for the group velocity horizon $x=x_0$ is represented as follows:

$$
\begin{cases}
\omega &= (v(x_0)+c_s(k(x_0)))k(x_0)\\
-v(x_0) &= \frac{\partial}{\partial k}(c_s^2(k)k^2)|_{k=k(x_0)}.
\end{cases}
\tag{D2}
$$

The first equation corresponds to the dispersion relation, and the second equation corresponds to the condition that two modes merge. Indeed, the second condition is the derivative of the dispersion relation at $k=k_0$. By deriving the first equation, we obtain

$$0=(v(x_0)+c_s(k(x_0)))+k(x_0)\left(v'(x_0)\left.\frac{dx}{dk}\right|_{k_0}+\left.\frac{\partial c_s}{\partial k}\right|_{k_0}\right). \tag{D3}$$

Now let us derive the approximate solution $k(x)$ of the dispersion relation corresponding to the Hawking mode at the vicinity of the group velocity horizon $x=x_0$. Assuming that Taylor expansion for $k(x)$ is possible about x_0, we can approximate $k(x)$ by

$$k(x)=k_0+\left.\frac{\partial k}{\partial x}\right|_{x_0}(x-x_0) \tag{D4}$$

$$\approx k_0\left(\frac{1}{1+v'(x_0)(x-x_0)/(v(x_0)+c_s(k_0)+k_0^2\partial c_s/\partial k|_{k_0})}\right). \tag{D5}$$

Here, we used the second equality of the (D2) and the formula of the Taylor expansion $(1+x)^{-1}\approx 1-x$. By using the first formula of the (D2) we can further simplify the equation,

$$k(x)\approx\frac{\omega}{\omega(\omega/k_0+v'(x_0)(x-x_0)+k_0\partial c_s/\partial k|_{k_0})/(\omega+k_0^2\partial c_s/\partial k|_{k_0})}. \tag{D6}$$

In the low frequency region, $c_s(k)\approx 1$ holds for the right-moving mode outside the group velocity horizon; therefore we can set $\partial c_s/\partial k|_{k_0}=0$ in this formula. We finally obtain

$$k(x)\approx\frac{\omega}{v'(x_0)(x-x_0)+\omega/k_0+k_0\partial c_s/\partial k|_{k_0}}. \tag{D7}$$

[1] S. W. Hawking, Particle creation by black holes, Commun. Math. Phys. **43**, 199 (1975); **46**, 206(E) (1976).
[2] S. W. Hawking, Black hole explosions, Nature (London) **248**, 30 (1974).
[3] J. D. Bekenstein, Black holes and entropy, Phys. Rev. D **7**, 2333 (1973).
[4] D. N. Page, Information in Black Hole Radiation, Phys. Rev. Lett. **71**, 3743 (1993).
[5] T. Jacobson, Black-hole evaporation and ultrashort distances, Phys. Rev. D **44**, 1731 (1991).
[6] R. Brout, S. Massar, R. Parentani, and P. Spindel, Hawking radiation without trans-Planckian frequencies, Phys. Rev. D **52**, 4559 (1995).
[7] W. G. Unruh, Experimental Black-Hole Evaporation?, Phys. Rev. Lett. **46**, 1351 (1981).
[8] W. G. Unruh, Sonic analogue of black holes and the effects of high frequencies on black hole evaporation, Phys. Rev. D **51**, 2827 (1995).
[9] W. G. Unruh and R. Schützhold, Universality of the Hawking effect, Phys. Rev. D **71**, 024028 (2005).
[10] U. Leonhardt and S. Robertson, Analytical theory of Hawking radiation in dispersive media, New J. Phys. **14**, 053003 (2012).
[11] S. J. Robertson, The theory of Hawking radiation in laboratory analogues, J. Phys. B **45**, 163001 (2012).
[12] S. Corley and T. Jacobson, Hawking spectrum and high frequency dispersion, Phys. Rev. D **54**, 1568 (1996).
[13] C. Mayoral, A. Fabbri, and M. Rinaldi, Steplike discontinuities in Bose-Einstein condensates and Hawking radiation: Dispersion effects, Phys. Rev. D **83**, 124047 (2011).
[14] S. Corley, Particle creation via high frequency dispersion, Phys. Rev. D **55**, 6155 (1997).
[15] S. Finazzi and R. Parentani, Hawking radiation in dispersive theories, the two regimes, Phys. Rev. D **85**, 124027 (2012).
[16] A. Coutant, R. Parentani, and S. Finazzi, Black hole radiation with short distance dispersion, an analytical *s*-matrix approach, Phys. Rev. D **85**, 024021 (2012).
[17] X. Busch and R. Parentani, Quantum entanglement in analogue Hawking radiation: When is the final state nonseparable?, Phys. Rev. D **89**, 105024 (2014).
[18] D. E. Bruschi, N. Friis, I. Fuentes, and S. Weinfurtner, On the robustness of entanglement in analogue gravity systems, New J. Phys. **15**, 113016 (2013).
[19] M. Isoard, N. Milazzo, N. Pavloff, and O. Giraud, Bipartite and tripartite entanglement in a Bose-Einstein acoustic black hole, Phys. Rev. A **104**, 063302 (2021).
[20] Y. Nambu and Y. Osawa, Tripartite entanglement of Hawking radiation in dispersive model, Phys. Rev. D **103**, 125007 (2021).
[21] P. Nation, M. Blencowe, A. Rimberg, and E. Buks, Analogue Hawking Radiation in a DC-Squid Array Transmission Line, Phys. Rev. Lett. **103**, 087004 (2009).
[22] P. Nation, J. Johansson, M. Blencowe, and F. Nori, Colloquium: Stimulating uncertainty: Amplifying the quantum vacuum with superconducting circuits, Rev. Mod. Phys. **84**, 1 (2012).
[23] S. Corley, Computing the spectrum of black hole radiation in the presence of high frequency dispersion: An analytical approach, Phys. Rev. D **57**, 6280 (1998).
[24] R. Schützhold and W. G. Unruh, Quantum correlations across the black hole horizon, Phys. Rev. D **81**, 124033 (2010).
[25] J. Steinhauer, Measuring the entanglement of analogue Hawking radiation by the density-density correlation function, Phys. Rev. D **92**, 024043 (2015).
[26] J. Fourdrinoy, S. Robertson, N. James, A. Fabbri, and G. Rousseaux, Correlations on weakly time-dependent transcritical white-hole flows, Phys. Rev. D **105**, 085022 (2022).
[27] L.-P. Euvé, F. Michel, R. Parentani, T. G. Philbin, and G. Rousseaux, Observation of Noise Correlated by the Hawking Effect in a Water Tank, Phys. Rev. Lett. **117**, 121301 (2016);
[28] D. A. Trunin, Particle creation in nonstationary large N quantum mechanics, Phys. Rev. D **104**, 045001 (2021).
[29] D. A. Trunin, Nonlinear dynamical Casimir effect at weak nonstationarity, Eur. Phys. J. C **82**, 440 (2022).
[30] E. Akhmedov, K. Bazarov, and D. Diakonov, Quantum fields in the future Rindler wedge, Phys. Rev. D **104**, 085008 (2021).
[31] E. T. Akhmedov, H. Godazgar, and F. K. Popov, Hawking radiation and secularly growing loop corrections, Phys. Rev. D **93**, 024029 (2016).
[32] A. Peres, Separability Criterion for Density Matrices, Phys. Rev. Lett. **77**, 1413 (1996).
[33] P. Horodecki, Separability criterion and inseparable mixed states with positive partial transposition, Phys. Lett. A **232**, 333 (1997).
[34] R. Simon, Peres-Horodecki Separability Criterion for Continuous Variable Systems, Phys. Rev. Lett. **84**, 2726 (2000).
[35] R. Simon, N. Mukunda, and B. Dutta, Quantum-noise matrix for multimode systems: U(n) invariance, squeezing, and normal forms, Phys. Rev. A **49**, 1567 (1994).
[36] G. Vidal and R. F. Werner, Computable measure of entanglement, Phys. Rev. A **65**, 032314 (2002).
[37] M. B. Plenio and S. Virmani, An introduction to entanglement measures, Quantum Inf. Comput. **7**, 1 (2007).